

A role for the otoliths in the mechanics of cochlear homeostasis?

Eric L. Le Page

Perth, Western Australia
ericlepage@innerearmechanisms.org

ABSTRACT

The role and function of the otolith organs might well hold continuing interest for those studying cochlear mechanics. The otoliths, utricle, saccule (and lagena in birds) are intriguing, not just because of their role in the evolutionary origins of inner ear function, but because, in mammals, their membranous structures are contained within the bony vestibule, directly in line with the action of the stapes[1]. Intriguingly they display highly-organised morphology[2]; [3]) and offer an apparently redundant low-frequency channel[4]. This duplication is puzzling considering cochlear low-frequency reception is generally less vulnerable than high. Unexplained is how pressures within the labyrinth are regulated[5]. A hypothesis is developed that the saccule's low-frequency pressure sensitivity may represent another function entirely, connected with the mechanics of cochlear homeostasis. A mathematical model is presented to illustrate how the otoliths may have two orthogonal modes, sensing otolith shear in differential mode, but sensing ambient pressure in common mode.

INTRODUCTION

This exercise therefore follows a long history of experiment, description and modelling of the otoliths [2, 6, 7] for which the popular objective has been understanding the sensing of gravity, movement and acceleration[8–12]. A new computational model is here presented for the function of an otolith organ, following interest in homeostatic regulation mechanisms centred on the endolymphatic system [5, 13]. Any regulatory mechanism for pressure should reasonably possess a pressure sensor, so where, within the membranous labyrinth is one located? The lagena is chosen for investigation because it seems to possess all the sensory pre-requisites. Being symmetric, it is less complex than either the saccule[10, 14] (and utricle) but possesses the same key property viz. centrifugal organisation of the hair cell orientation[12, 15].

The layers of the otolithic membrane are important for the model. Immediately above the sensory macula containing the hair cells are three layers. The first is a gel layer which is elastic [16] through which the hair bundle and kinocilia pass. Next there is a stiffer mesh-layer into which the tips of the kinocilia are anchored[16]. Finally, above this sits the inertial otoconia layer which is elastic because the otoconia themselves are separated by gel[17].

This model calculates the motions of kinocilia with their roots anchored in the macula, given motion which is numerically applied to the whole otolith surface. Such motion is not limited to just shear. It stems from the realisation that the elasticity leaves open another mode – force normal to the macular surface acting upon the balloon-like properties of the otolithic membrane.

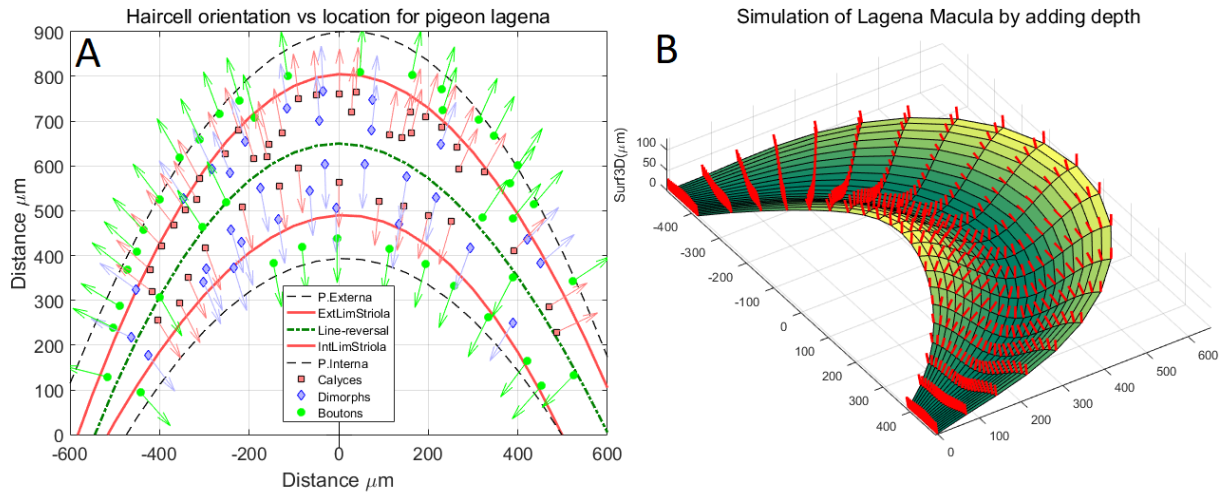


Figure 1A. The lagenar macula has similar cell polarization with the saccular macula -- the cells are maximally sensitive along lines directed radially away from the line-of-reversal (green, dashed). The figure is redrawn from M. Zakir et al. 2013, Fig. 3 and curve fits in polar coordinates are used to form the model. The striola region, approximately between the curved red lines, contains predominantly phasic calyx hair cells. The extra-striola region lies along the rims of the structure and contains predominantly type II cells with bouton endings giving a tonic response. The 3d form of the macular surface (Panel B) was chosen to explore the basis of the centrifugal organization. The hair cells are organized to be equally-spaced on a polar mesh grid with their kinocilia normal to the surface, shown in red.

Assumptions

Movements of the otoconia layer cause a corresponding change in angle of the kinocilia tracking the position of the otolith. Secondly, the elastic gel matrix acts as a compression spring which holds the kinocilia under some minimal tension keeping them taut and linear. It also allows anisotropic distribution of stimulation capitalising on the nonplanar macula. Movement applied is not resisted by changes in tension of the kinocilia. Boltzmann statistics for hair cell stimulation are not invoked for lack of detailed morphological information.

METHODS

MATLAB™ (v2016b) is used to simulate otolith function. The basic shape of the lagena is taken from curve fits of the morphology [18] redrawn in Fig.1A. Hair cells external to the so-called line-of-reversal (green dashed line) are oriented towards the longer rim (pars externa), and vice versa. The 2d map immediately suggests that the macula is not planar but that the reversal of polarity makes sense if the opposite sides of the line-of-reversal are in reality opposing flanks of a ridge or valley. Accordingly, the height variation is chosen as

$$H(r, \theta) = A \cos(r) \operatorname{sech}(\theta)$$

where $0 < r \leq 2\pi$ for a ridge (or alternately $-\pi < r \leq \pi$ for a valley) and $-\pi < \theta \leq \pi$. (Fig.1B). Each polar dimension is scaled to vary with the boundary values of radii, also the angular span of the lagena from values from the curve fits to Fig1A. The line-of-reversal runs along the curved bottom of the valley and the striola is situated on the opposing slopes of the valley. Conversely, the extra-striola region lies in the hilltops above the valley. Due to the otolith elasticity both regions receive a very different manner of stimulation from the applied movement. The stretching of the membrane radially means that both sides move in phase in the z direction.

This macular surface is generated using a polar mesh grid. One hair cell and the rootlet of its kinocilium is assumed located at every intersection of the meshgrid and are thus equally distributed along each dimension. A corresponding second grid is computed for the kinocilium tips over their roots, calculated by assuming the length of all the kinocilia may have values from $15\mu\text{m}$ [19] to $80\mu\text{m}$ [20]. Thus, the matrix of 3d positions of the kinocilia tips define the otoconia surface which is treated as another object. Each hair cell has an optimal angle of sensitivity defined in our case as discrete values of θ for the unstimulated case – for which each kinocilium is assumed to stand normal to the surface (Fig.1B).

Stimulating the otolith involves computing the new positions of the kinocilia tips, by applying 3d affine transformations (translation and scaling) for each point in the xy-stimulus sequence.

Translation by $T(xyz)$ $T_c = \begin{bmatrix} 1 & 0 & 0 & T(x) \\ 0 & 1 & 0 & T(y) \\ 0 & 0 & 1 & T(z) \\ 0 & 0 & 0 & 1 \end{bmatrix}$	Scaling by $S(xy)$ $S_a = \begin{bmatrix} S & 0 & 0 & 0 \\ 0 & S & 0 & 0 \\ 0 & 0 & 1 & 0 \\ 0 & 0 & 0 & 1 \end{bmatrix}$
Combined affine transformation: $M = S_a * T_c$	

Table 1 Movement of the otoconial membrane mass is simulated by applying 3d affine transformations to the coordinates of the kinocilia tips. Unstimulated, these are calculated to be normal to the surface at the locations of the kinocilia roots, but distant by the length of the kinocilia. Translation by T tests shear, while scaling by S explores the surface elasticity of the gel-matrix.

positions, while the height value (z) represents the deflection ϕ in degrees. Since deflection either side of the optimal direction would result in less depolarisation, the norm of the cross product is taken. This rectification means that $z \geq 0$ for all cells. At local places on the lagena where any kinocilium is currently at the cell's optimal angle (normal to the surface), the height of the deflection surface is zero degrees. By definition, for no applied stimulus, the whole lagena response is a surface coincidental with the xy-plane. The height of the deflection surface depends upon the expansion factor $S \in (1.05, 1.4)$ as does the sharpness of the notch.

RESULTS

Affine transformation resulting in otolith shear being detected by the striola

Figure 2 shows for any centroid, chosen here to be situated on the reversal line, points either side move radially in *opposite* directions thus directly capitalising on the centrifugal organisation, while their z components move in the *same* direction. The key result is that there is a defined region (red patch) of minimal deflection. This appears as a notch in the 3d surface. As the otolith executes the movement in the xy-plane, the location of the notch moves within the region defined by the flanks of the valley as shown, $x, y \in [-40, +80]$. The deflection surface is shown in Fig.2B and 2D from different viewpoints. The notch shows that somewhere on the surface a kinocilium is perfectly aligned with the orientation of the cell. As the otoconia move, shear produces a localised rapid change in deflection within striola region. The notch traces the

Having obtained a new otolith surface, the new set of kinocilia vectors is defined by taking the vector differences of the roots from the tips. The kinocilia deflections ϕ from their normal positions are given by

$$\phi = \tan^{-1} (\|v_1 \otimes v_2\| \cdot v_1 \odot v_2), \forall v_1, v_2,$$
where v_1 are the kinocilia in resting positions, v_2 in stimulated positions, at each point in time.

The output of the model is, for each kinocilium on the meshgrid, the value ϕ relative to its orientation which varies as θ . This set of deflections is displayed as a 3d surface, where the xy-values are taken as the kinocilia root

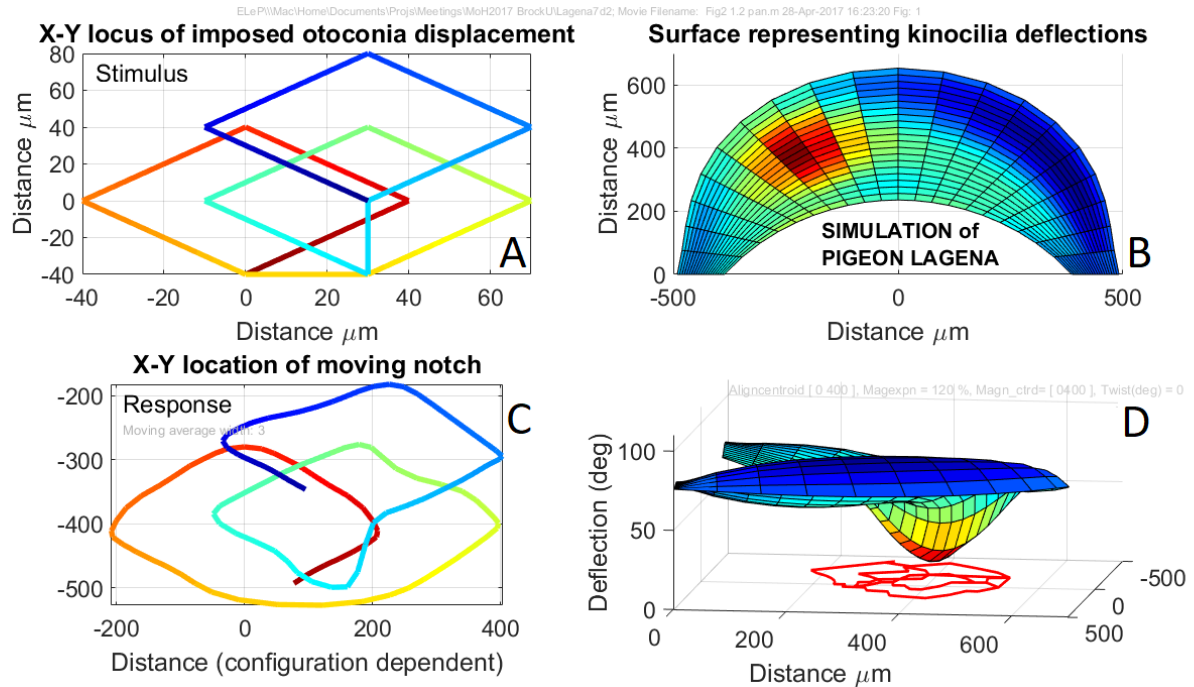


Figure 2 A simulation of the deflection of the field of kinocilia in the pigeon lagena for a pseudo-random-walk X-Y stimulus applied to the otoconia. In the two views on the right of the colored surface the Z axis gives the global picture of deflections of all the kinocilia from the angle of their respective optimal orientation. As the otoconial membrane moves relative to the macula a prominent single notch is formed as a localized patch of hair cells swing through zero deflection. The resulting response locus is found from a planar search for the notch, result slightly smoothed. The response is effectively a topographic map of inertial movement of the otolith, which is mostly detected by the calyces and dimorphs of the striola, differentiated by phasic response.

movement of the otolith with reasonable fidelity of the stimulus (Fig.2C and 2D). The model suggests that the lagena can deliver a topographic representation of shear movement.

Affine transformation exploring elasticity of the gel-matrix

Figure 3 shows the effect of varying the expansion factor for two values, 0.9 and 1.1 (Panels A and B). The x-y position of the otolith is fixed in relation to the macula. The extra-striola regions on the lagena are most sensitive to stretch of the gel-matrix (radially furthest from the line-of-reversal). This effect is attributed to the centrifugal organisation of the hair cells because the deflections on opposite sides are both resulting in depolarisation. Neural detection of hydrostatic pressure may be achieved by extracting the common mode deflections for opposite hilltops. Expansion from unity produces a positive-going deflection, while contraction produces a negative going deflection. The reversal of colours either side of unity is deliberate because deflections rapidly traverse zero at unity. The polarity of the movement tracking is also reversed.

DISCUSSION

The property of interest here is that the 3d topology of the maculae may be vital to connect their morphology with function. The adopted form of the model is consistent with expected dynamic behaviours attributed to the phasic cells of the striola[15], effectively differentiating the

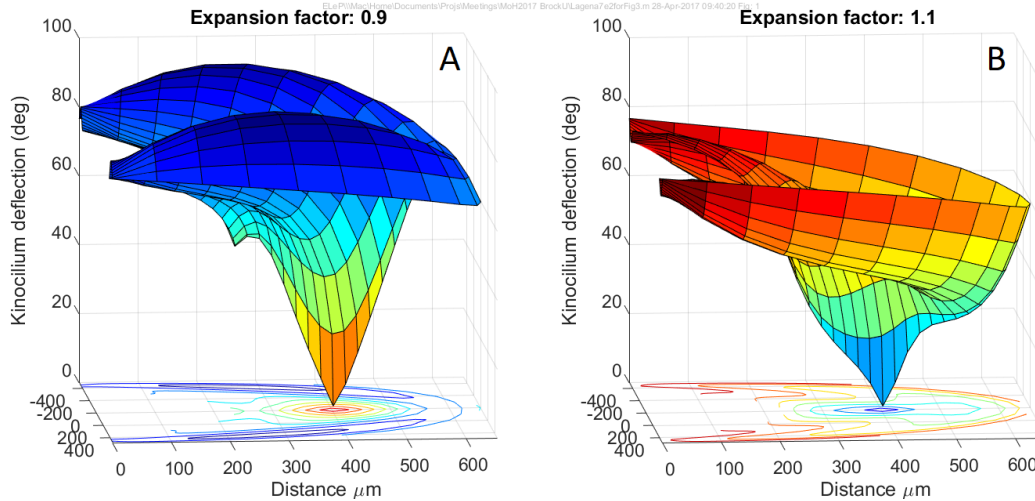


Figure 3 The otolithic membrane has its dense otoconia embedded in a gel matrix. The membrane is elastic. This simulation tests the effect of varying the amount of stretch of the membrane, say as might be due to variation of hydrostatic pressure. Varying the expansion factor (0.9 Panel A, 1.1 Panel B) has a profound effect upon deflections at the rims of the lagena in the extra-striola region where the type II cells give a tonic response. The boutons have high firing rates so they could appropriately register a drop in pressure as well as rise (see Discussion).

displacement of the inertial otoconial mass. Conversely, the extra-striola region is most heavily populated by the type II hair cells with their bouton nerve endings and tonic firing behaviour[12].

Points either side of the line-of-reversal can move in opposite directions, thereby making sense of the centrifugal organisation, allowing for innervation to be organised to sense common mode as well as a differential mode. Vestibular median discharge rates are over 50/s [12]. Conversely it capitalises on the notion that the otolithic membrane may stretch by various amounts suggesting expansion and contraction could monitor endolymph pressure. Future effort to develop the model would warrant attention to test constraints imposed by the tip attachments and the nature of a neural net for efferent control of water shunting between cochlear compartments[21]. Quite apart from their roles in management of balance, they also contain the pre-requisites to register static pressure[22].

Significance and predictions

Otolith science has been strongly directed at using the shear mode to explain balance. It will be found that the vestibular neural response will support a second mode: pressure sensitivity. Both variables appear to be orthogonal – shear is sensed in differential mode while the common mode deflections will carry the information about ambient pressure. Secondly, the utricle and saccule likely function in tandem as the control element in an osmotically-driven homeostatic management system [21] which has evolved to cope with ambient pressure change. Since the proposed common mode scheme cannot support expansion factors of unity, and since hair cell polarity in the utricle is reversed in the saccule, it will be found that the nature of the tandem operation will be analogous to an electronic amplifier operating in Class B (with overlap). Lastly, the study of cochlear mechanics has been complicated by lack of knowledge of this mechanism which, under conditions of high sensitivity and sharp tuning obscures its own existence, viz. the 2-chamber model may be perfectly adequate while this active mechanism is dormant but is challenged by ambient pressure change or efferent[23] or other experimental disturbances[24].

REFERENCES

1. Zhang T-Y, Dai P-D, Wang Z-M, Wang K-Q, Chen JX, Xie L (2007) A contour map of the ear's vestibular apparatus based on 3D reconstruction. *Computing in Science & Engineering* 9:26–31
2. Jaeger R, Kondrachuk A, Haslwanter T (2008) The distribution of otolith polarization vectors in mammals: comparison between model predictions and single cell recordings. *Hearing research* 239:12–19
3. Uzun-Coruhlu H, Curthoys IS, Jones AS (2007) Attachment of the utricular and saccular maculae to the temporal bone. *Hearing research* 233:77–85
4. Todd N (2001) Evidence for a behavioral significance of saccular acoustic sensitivity in humans. *The Journal of the Acoustical Society of America* 110:380–390
5. LePage E, Avan, P. (2015) Direct Testing of the Biasing Effect of Manipulations of Endolymphatic Pressure on Cochlear Mechanical Function. In: K. Domenica Karavitaki and David P. Corey (ed) 12th Mechanics of Hearing Workshop, Cape Sounio, Greece June23-29, 2014. *AIP Conf. Proc.* 1703, (2015), pp 417–421
6. Kondrachuk A (2006) Modeling of mechanical stimulation of hair cells in otolithic organs. *Advances in Space Research* 38:1052–1056
7. Ladich F, Popper AN (2004) Parallel evolution in fish hearing organs. *Evolution of the vertebrate auditory system*. Springer, pp 95–127
8. Kondrachuk AV (2002) Otoliths as biomechanical gravisensors. *Adv Space Res* 30:745–50
9. Popper AN, Fay RR, Platt C, Sand O (2003) Sound detection mechanisms and capabilities of teleost fishes. *Sensory processing in aquatic environments*. Springer, pp 3–38
10. Ladich F, Schulz-Mirbach T (2016) Diversity in fish auditory systems: one of the riddles of sensory biology. *Frontiers in Ecology and Evolution* 4:28
11. Popper AN, Schilt CR (2008) *Hearing and acoustic behavior: basic and applied considerations*. Fish bioacoustics. Springer, pp 17–48
12. Fernandez C, Goldberg JM (1976) Physiology of peripheral neurons innervating otolith organs of the squirrel monkey. I. Response to static tilts and to long-duration centrifugal force. *J. Neurophysiology* 39:970–984
13. LePage E, Olofsson Å (2011) Modeling Scala Media as a Pressure Vessel. *AIP Conference Proceedings, What Fire is in Mine Ears: Progress in Auditory Mechanics*. p 212-217
14. Schulz-Mirbach T, Ladich F, Plath M, Metscher BD, Heß M (2014) Are accessory hearing structures linked to inner ear morphology? Insights from 3D orientation patterns of ciliary bundles in three cichlid species. *Frontiers in zoology* 11:1
15. Goldberg JM, Lysakowski A, Fernández C (1992) Structure and Function of Vestibular Nerve Fibers in the Chinchilla and Squirrel Monkey. *Annals of the New York Academy of Sciences* 656:92–107
16. Jaeger R, Takagi A, Haslwanter T (2002) Modeling the relation between head orientations and otolith responses in humans. *Hearing research* 173:29–42
17. Kniep R, Zahn D, Wulfes J, Walther LE (2017) The sense of balance in humans: Structural features of otoconia and their response to linear acceleration. *PLOS ONE* 12:e0175769
18. Zakir M, Wu L-Q, Dickman JD (2012) Morphology and innervation of the vestibular lagena in pigeons. *Neuroscience* 209:97–107
19. Lewis E, Nemanic P (1972) Scanning electron microscope observations of saccular ultrastructure in the mudpuppy (*Necturus maculosus*). *Cell and Tissue Research* 123:441–457
20. Xue J, Peterson EH (2006) Hair bundle heights in the utricle: differences between macular locations and hair cell types. *J Neurophysiol* 95:171–86
21. Hirt B, Penkova Z, Eckhard A, Liu W, Rask-Andersen H, Müller M, Löwenheim H (2010) The subcellular distribution of aquaporin 5 in the cochlea reveals a water shunt at the perilymph-endolymph barrier. *Neuroscience* 168:957–970
22. Dinh TAD, Haasler T, Homann G, Jüngling E, Westhofen M, Lückhoff A (2009) Potassium currents induced by hydrostatic pressure modulate membrane potential and transmitter release in vestibular type II hair cells. *Pflügers Archiv-European Journal of Physiology* 458:379–387
23. Cooper NP, Guinan JJ (2006) Efferent-mediated control of basilar membrane motion. *J Physiol (Lond)* 576:49–54
24. LePage EL (1987) Frequency-dependent self-induced bias of the basilar membrane and its potential for controlling sensitivity and tuning in the mammalian cochlea. *J. Acoust. Soc. Amer.* 82:139–154